

Vortex creation in a trapped Bose-Einstein condensate by stimulated Raman adiabatic passage

G. Nandi,* R. Walser, and W. P. Schleich

Abteilung für Quantenphysik, Universität Ulm, D-89069 Ulm, Germany

(Received 16 January 2004; revised manuscript received 5 April 2004; published 10 June 2004)

We examine a scheme for the optical creation of a superfluid vortex in a trapped Bose-Einstein condensate, using the stimulated Raman adiabatic passage technique (STIRAP). By exposing an oblate, axis-symmetric condensate to two copropagating laser pulses, one can transfer external angular momentum from the light field to the matter wave, if one of the beams is the fundamental Gaussian mode and the other is a Gauss-Laguerre mode of angular momentum $1\hbar$. We demonstrate the complete transfer efficiency by numerical integration of the multicomponent Gross-Pitaevskii equation and explain the results with an intuitive and accurate approximation within the Thomas-Fermi limit. In addition, we discuss residual excitations (breathing modes) which occur in the two-dimensional regime and present the Bogoliubov excitation spectrum.

DOI: 10.1103/PhysRevA.69.063606

PACS number(s): 03.75.Lm, 03.75.Kk, 03.75.Mn

I. INTRODUCTION

Ultracold atomic gases have provided us with novel physical systems that exhibit all genuine many-body phenomena known from traditional condensed matter physics and, still, admit all the superior coherent control tools used in quantum optics. After the experimental realization of a Bose-Einstein condensate (BEC) itself, tremendous efforts were focused on the creation of topological and solitary excitations of condensates (for a current review see Ref. [1]). Especially alternative methods for the creation of vortices have stirred the minds, as the traditional “rotating-the-squeezed-bucket” procedure was not successful, initially. Thus, the first fruitful proposal to create a vortex involved a rapidly rotating Gaussian laser beam entangling the external motion with internal state Rabi oscillations [2,3]. Later, condensates were stirred up mechanically [4–6] and evaporative spin-up techniques created vorticity [7] and recently giant vortices [8] could be created. Due to larger asymmetries in the trapping potentials that can be achieved nowadays, vortices are now predominantly created with the stirring method and fascinating Abrikosov lattices containing up to 300 vortices have been made [6,9,10]. Alternatively, prospects for creating vortices by optical phase imprinting [11] were investigated (in analogy to the successful soliton experiment [12]) and applying magnetic interactions were considered [13]. Moreover, there have been ideas to create vorticity by sweeping a laser beam on a spiraling trajectory across the trap, inducing a Landau-Zener transition between the irrotational and the rotational state [14].

On the other hand, the transfer of angular momentum from an optical field to a macroscopic rigid body or an atomic particle has also a long standing tradition in quantum mechanics. The first proof that circularly polarized light carries angular momentum dates back to Beth’s original experiment of 1936 [15]. More recently, due to the availability of Gauss-Laguerre laser beams with well-defined external angular momentum [16,17] it is possible to use them as optical

tweezers and twistors [18–20]. Surprisingly, even the transfer of angular momentum to ultrasonic waves in fluids can be achieved that way [21]. In the context of a BEC, using the angular momentum of light to create a doubly charged vortex has been proposed [22], π pulses in Raman type transitions were examined [23] and an adiabatic passage to a vortex state was investigated by changing the two-photon detuning of an effective two-level system [24].

In this paper, we will examine the transfer of external angular momentum of light to the matter wave with the help of a stimulated Raman adiabatic passage (STIRAP) [25]. The basic effect relies on a quantum mechanical interference between two ground states and gives rise to a multitude of physical phenomena, e.g., dark resonances in optical spectroscopy [26], velocity selective coherent population trapping (VSCPT) [27], a drastic modification of the optical index of refraction (EIT) of normal [28] and BE condensed systems [29,30], as well as constructive procedures to prepare [31] and readout quantum states of atomic beams and optical cavities [32].

This paper is organized as follows: In the Sec. II we will develop a scheme for creating a vortex in a BEC using the STIRAP method. In analogy to single-particle physics, it is possible to derive the relevant three-component Gross-Pitaevskii equation. In Sec. III we will present the results of numerical calculations that are in good agreement with a simple analytical approximation within the Thomas-Fermi limit. In addition, we will discuss the physics of the remaining residual excitations in terms of the “breathing modes” of a quasi-two-dimensional system. In particular, we will calculate the radial Bogoliubov excitation spectrum of a condensate in the vortex state with angular momentum $1\hbar$. Finally, we will summarize our results and conclude in Sec. IV.

II. STIRAP IN A BOSE-EINSTEIN CONDENSED GAS

The STIRAP method is now applied to a trapped BEC of three-level atoms in a Λ -type configuration shown in Fig. 1. The two internal electronic ground states, e.g., the hyperfine levels of an alkali atom [29,33,34], are denoted by $|b\rangle$ and

*Electronic address: gerrit.nandi@physik.uni-ulm.de

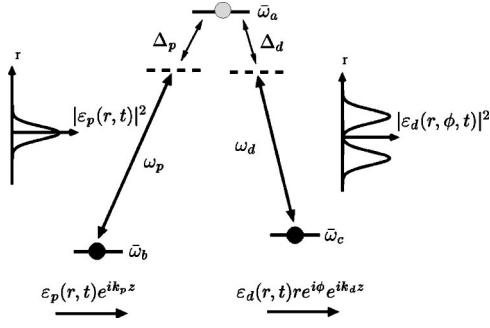


FIG. 1. A Λ -system exposed to two copropagating laser pulses in two-photon resonance. The atomic transition frequencies are Doppler-shifted with respect to the rest frame i.e., $\bar{\omega}_a = \omega_a + \hbar k_p^2/2M$, $\bar{\omega}_b = \omega_b$, $\bar{\omega}_c = \omega_c + \hbar(k_p - k_d)^2/2M$. Only one Gauss-Laguerre laser beam (ϵ_d) carries $1\hbar$ of angular momentum. The individual detunings from the excited state are $\Delta_p = \bar{\omega}_a - \bar{\omega}_b - \omega_p$, $\Delta_d = \bar{\omega}_a - \bar{\omega}_c - \omega_d$.

$|c\rangle$, and by absorbing an optical photon, one reaches the excited state $|a\rangle$, respectively. The condensate is confined spatially by an oblate, axis-symmetric harmonic potential, which reads in cylindrical coordinates (r, ϕ, z) ,

$$V(r, z) = \frac{1}{2}M(\omega^2 r^2 + \omega_z^2 z^2), \quad (1)$$

where M denotes the single-particle mass. By choosing the radial trapping frequency much less than the longitudinal frequency, i. e., $\omega \ll \omega_z$, one can confine the motion effectively to the radial component.

Now, we will expose the dilute atomic gas to two copropagating traveling “pump” and “dump” laser pulses,

$$\mathbf{E}_p(z, t) = \boldsymbol{\lambda}_p \epsilon_p(t) e^{-i(\omega_p t - k_p z)} + \text{c.c.}, \quad (2)$$

$$\mathbf{E}_d(r, \phi, z, t) = \boldsymbol{\lambda}_d \epsilon_d(r, \phi, t) e^{-i(\omega_d t - k_d z)} + \text{c.c.}, \quad (3)$$

where $\boldsymbol{\lambda}_p$ and $\boldsymbol{\lambda}_d$ denote the corresponding polarization vectors. The slowly varying laser beam envelopes ϵ_p , ϵ_d have a nontrivial temporal and spatial structure,

$$\epsilon_p(r, t) \approx \epsilon_p(t) = \epsilon_p e^{-(t - \tau)^2/2 d^2}, \quad (4)$$

$$\epsilon_d(r, \phi, t) \approx \epsilon_d r e^{i\phi} e^{-r^2/2 d^2}. \quad (5)$$

For the pump pulse, we choose the fundamental Gauss-Laguerre (GL) laser mode [16] with a spatial width larger than the BEC size and a temporal Gaussian turn-on shape with the width d . Numerical simulations prove that in this limit the spatial Gaussian envelope can be disregarded altogether in Eqs. (4) and (5). This pulse reaches its maximum intensity at some time $\tau > 0$. In order to transfer orbital angular momentum from the light beam to the matter wave, we pick the first excited GL mode that carries external angular momentum, the so-called “doughnut-mode,” for the dump beam [17,18,22,23]. While spatial extension and temporal duration d can be set equal in both pulses, it is crucial that the dump beam reaches its maximum intensity at $t=0$, first. This “counter-intuitive” pulse sequence is the key of the STIRAP procedure and achieves an efficient adiabatic passage

for linear, dissipative quantum systems [25,27,32]. A full population transfer can be reached if the field amplitudes satisfy the conditions

$$\lim_{t \rightarrow -\infty} \frac{\epsilon_p(t)}{\epsilon_d(t)} = 0, \quad (6)$$

$$\lim_{t \rightarrow +\infty} \frac{\epsilon_p(t)}{\epsilon_d(t)} = \infty, \quad (7)$$

which is guaranteed by the pulse sequence given in Eqs. (4) and (5).

Far below the transition temperature $T \ll T_{\text{BEC}}$, one can describe a multicomponent BEC effectively within a simple mean-field picture [35,36]. Thus, we introduce a three component state vector $\boldsymbol{\Psi}(\mathbf{r}, t)$, that represents the components of the macroscopic atomic matter wave. For the time evolution of this multilevel state vector, one can derive a generalized Gross-Pitaevskii (GP) mean-field equation [37]

$$\boldsymbol{\Psi}(\mathbf{r}, t) = (\Psi_a(\mathbf{r}, t), \Psi_b(\mathbf{r}, t), \Psi_c(\mathbf{r}, t))^T, \quad (8)$$

$$i\hbar \partial_t \boldsymbol{\Psi}(\mathbf{r}, t) = H(t) \boldsymbol{\Psi}(\mathbf{r}, t). \quad (9)$$

$\boldsymbol{\Psi}(\mathbf{r}, t)$ is normalized to the total particle number,

$$N = \int d^3r (|\Psi_a(\mathbf{r}, t)|^2 + |\Psi_b(\mathbf{r}, t)|^2 + |\Psi_c(\mathbf{r}, t)|^2), \quad (10)$$

in the BEC. Due to the unitarity of Eq. (9), this particle number is conserved at all times. However, as we use explicitly time-dependent laser fields, the energy of the system can change (see Sec. III B).

The internal structure of the Hamiltonian is quite easy to understand, as it follows straight from the single-particle physics that rules the dynamics of the dilute gas interacting with light. In Fig. 1, we have depicted the optical dipole transition scheme for a Λ -type atom. Within the standard rotating-wave approximation of quantum optics, [39] one finds for the internal state Hamiltonian

$$H(t)/\hbar = \begin{pmatrix} h_a + \Delta & \Omega_p(t) & \Omega_d(r, \phi, t) \\ \Omega_p^*(t) & h_b + \delta & 0 \\ \Omega_d^*(r, \phi, t) & 0 & h_c - \delta \end{pmatrix}. \quad (11)$$

The Rabi frequencies $\Omega_p(t) = \epsilon_p(t) d_{ba}/\hbar$ and analogously $\Omega_d(r, \phi, t) = \epsilon_d(r, \phi, t) d_{ca}/\hbar$, measure how well the photon field couples to the electronic transition and are proportional to the atomic dipole moments d_{ba} , d_{ca} . The remaining parameters are the Raman detuning $\Delta = (\Delta_p + \Delta_d)/2$ and the two-photon detuning $\delta = (\Delta_d - \Delta_p)/2$, which refer to the individual detunings Δ_p , Δ_d of the laser frequency and the Doppler-shifted electronic transition frequency. In order to achieve the optimal STIRAP performance, we will assume a two-photon resonance condition $\delta=0$ later, and pick a nonvanishing detuning Δ in order to avoid detrimental spontaneous emissions, which would disrupt the coherent evolution. In the preceding derivation of Eq. (11), we have also tacitly adopted co-moving and co-rotating reference frames such that

$$\bar{\Psi}(\mathbf{r}, t) = (e^{i[(\bar{\omega}_a - \Delta)t - k_p z]} \Psi_a(\mathbf{r}, t), e^{i(\bar{\omega}_b - \delta)t} \Psi_b(\mathbf{r}, t), e^{i[(\bar{\omega}_c + \delta)t - (k_p - k_d)z]} \Psi_c(\mathbf{r}, t))^T, \quad (12)$$

in order to strip off the trivial plane wave character of the beams, see Eqs. (2) and (3). To keep the notation simple, we will drop the bar over the state vector in the following discussion.

For the external motion of the multicomponent gas, we want to assume that all components are confined by the same harmonic potential, cf. Eq. (1). This is not a stringent requirement for the excited state component Ψ_a , as particles will only rarely occupy this level and move through it quickly. Due to this low occupancy, it is also not necessary to consider any mean-field shifts arising from self-interaction, or the motion through the remaining components. Consequently, we can simply use the bare trap Hamiltonian with a Doppler shift

$$\hbar h_a = \frac{\mathbf{p}^2}{2M} + V(r, z) + \hbar k_p \frac{p_z}{M}. \quad (13)$$

For the ground state components, we will only consider mean-field shifted energy contributions that arise from elastic collisions and denote the interspecies and intraspecies scattering lengths by $\{a_{bb}, a_{bc}, a_{cb}, a_{cc}\}$. Hence, these components read

$$\hbar h_b = \frac{\mathbf{p}^2}{2M} + V(r, z) + \frac{4\pi\hbar^2}{M} (a_{bb} |\Psi_b|^2 + a_{bc} |\Psi_c|^2), \quad (14)$$

$$\hbar h_c = \frac{\mathbf{p}^2}{2M} + V(r, z) + \hbar(k_p - k_d) \frac{p_z}{M} + \frac{4\pi\hbar^2}{M} (a_{cc} |\Psi_c|^2 + a_{cb} |\Psi_b|^2). \quad (15)$$

The optical absorption-emission cycle imparts angular, as well as linear momentum onto the final state matter-wave Ψ_c . However, linear momentum cannot be conserved in a trapped system, and it would lead to a sloshing motion along the z direction. This can be suppressed either, by choosing equal laser frequencies and photon momenta, or by squeezing the trapping potential into a very oblate configuration such that $\beta = \omega_z / \omega \gg 1$. This effectively “freezes” the longitudinal motion due to an energy selection argument.

The later situation leads to a more stable configuration and is favorable. Thus, we are able to approximate the state vector

$$\Psi(\mathbf{r}, t) = (\psi_a(r, t), \psi_b(r, t), e^{-i\phi} \psi_c(r, t))^T \varphi_0(z, t), \quad (16)$$

by factorizing it into a radial part, which is normalized to the number of particles in the BEC, i.e.,

$$N = 2\pi \int_0^\infty dr r (|\psi_a|^2 + |\psi_b|^2 + |\psi_c|^2), \quad (17)$$

and the ground state

$$\varphi_0(z, t) = (\beta/\pi)^{1/4} e^{-i\beta t/2} e^{-\beta z^2/2} \quad (18)$$

of the one-dimensional harmonic oscillator in the z direction, which is normalized to one, i.e.,

$$\int_{-\infty}^{\infty} dz |\varphi_0|^2 = 1. \quad (19)$$

Please note that the third component now carries the mechanical angular momentum of $1\hbar$ per particle. After projecting the state vector along the z direction, we finally arrive at an effective Hamiltonian in the radial direction. Using the natural units of the transverse harmonic oscillator (time unit $T_{\text{HO}} = 2\pi/\omega$, length scale $a_{\text{HO}} = \sqrt{\hbar/M\omega}$), one finds

$$i\partial_t \psi(r, t) = H(t) \psi, \quad (20)$$

$$H(t) = \begin{pmatrix} h^{(0)} + \Delta & \Omega_p(t) & r \Omega_d(t) \\ \Omega_p^*(t) & h^{(0)} + \delta + \kappa n(r) & 0 \\ r \Omega_d^*(t) & 0 & h^{(1)} - \delta + \kappa n(r) \end{pmatrix}, \quad (21)$$

where $\kappa = \sqrt{8\pi\beta} a$ and all scattering lengths are equal to a . This assumption holds well for ^{87}Rb (see below). The particle density is denoted by $n(r) = |\psi_b(r)|^2 + |\psi_c(r)|^2$, and $h^{(m)}$ represents a two-dimensional radial harmonic oscillator Hamiltonian

$$h^{(m)} = -\frac{1}{2} \left(\partial_r^2 + \frac{1}{r} \partial_r - \frac{m^2}{r^2} - r^2 \right) \quad (22)$$

in an angular momentum manifold with $m \leq 0$.

III. RESULTS AND DISCUSSION

In the following, we will be more specific and choose the typical scattering parameters for ^{87}Rb [33,34]. To simplify matters, we will also assume that the self-scattering and cross-component scattering lengths are equal: $a_{bb} = a_{cc} = a_{bc} = a = 110$ Bohr radii (a_0). This turns out to be a very robust approximation and we comment on this later. By implementing a numerical algorithm for solving the three-component Gross-Pitaevskii equation (20), we can show that a quantized vortex ($m=1$) is building up. For the trap frequencies we choose $\omega = 2\pi \times 10 \text{ s}^{-1}$ and $\omega_z = 2\pi \times 1000 \text{ s}^{-1}$, respectively. With an atomic mass of $M = 86.91$ amu, we find a harmonic oscillator size $a_{\text{HO}} = \sqrt{\hbar/M\omega} = 3.41 \mu\text{m}$. In this spatial unit, we get for the scaled coupling constant $\kappa = \sqrt{8\pi\beta} a = 0.0855$. We will consider an atomic ensemble with $N = 10\,000$ particles. From a simple Thomas-Fermi approximation [see Eq. (29)] one finds estimates for the condensate radius $R_{\text{TF}} = \sqrt{2\mu_{\text{TF}}} = 5.7$ with a chemical potential $\mu_{\text{TF}} = 16.5$. The laser parameters are chosen as follows: $\tau = 0.3$, $d = 0.15$, $\Omega_p = 200$, $\Omega_d = 200$, $\Delta = 30$, and $\delta = 0$ (two-photon resonance). In prac-

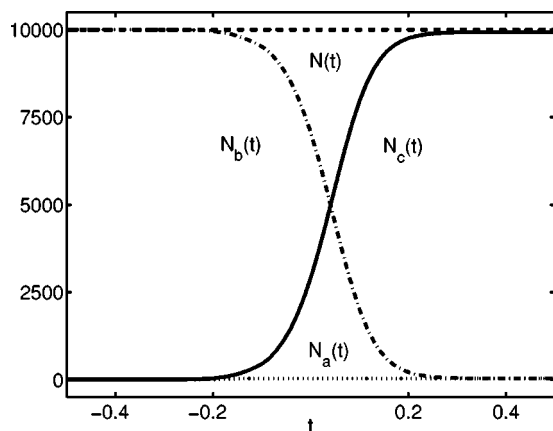


FIG. 2. Time evolution of the individual level populations vs time measured in natural units of T_{HO} . The dotted line depicts the population $N_a(t)$ of the excited state, the dashed-dotted and the solid lines represent $N_b(t)$ and $N_c(t)$, respectively, and the dashed line corresponds to the total number of particles in the system, which is conserved, i.e., $N(t) = N_a(t) + N_b(t) + N_c(t)$.

tice, Δ will be of the order of at least 10^5 , but for the simulations much lower values are sufficient.

In Fig. 2 the transfer efficiency is demonstrated. Initially the whole system is prepared in the ground state $|b\rangle$. While the excited state $|a\rangle$ is not populated significantly at any instant, the population of state $|c\rangle$ is rising up. An almost 100% transfer to the vortex state is possible and the total number of particles in the BEC is conserved as required by unitarity. The time evolution of the vortex state density is shown in Fig. 3. At some intermediate time ($t=0$) high-frequency excitations appear. After the transfer is completed ($t=1$), the shape of a vortex with angular momentum $1\hbar$ is matched almost perfectly with the stationary single charged vortex solution. Still, some minor excitations, i.e., the “breathing mode” remains, which will be discussed in Sec. III B. In Fig.

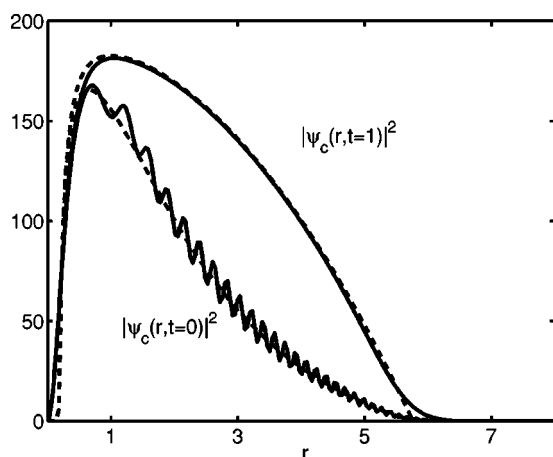


FIG. 3. Time evolution of the vortex state density $|\psi_c(r,t)|^2$ vs radius r measured in units of a_{HO} . The solid lines depict the vortex state at an intermediate instant ($t=0$) and after the STIRAP process is completed ($t=1$). In general, the instantaneous Thomas-Fermi approximation (dashed line) compares well with the exact results apart from minor excitations.

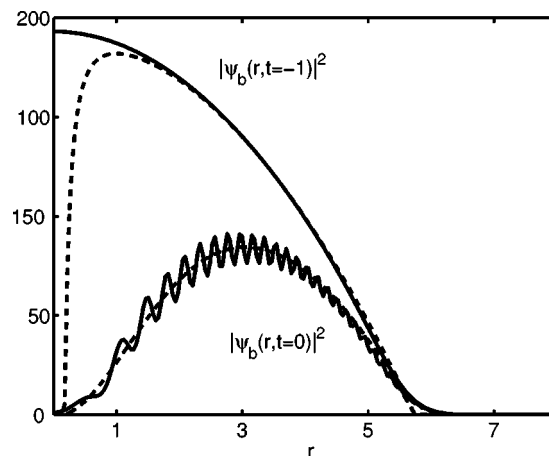


FIG. 4. Time evolution of the irrotational state density $|\psi_b(r,t)|^2$ vs radius r measured in units of a_{HO} . The solid lines depict the position density at the initial ($t=-1$) and at some intermediate time ($t=0$). The instantaneous Thomas-Fermi approximation (dashed lines) matches the exact solution after the transfer of particles started effectively ($t \geq 0$).

4, we demonstrate the time evolution of the density of the irrotational state $|b\rangle$. Initially, the atoms of the condensate are prepared in the ground state ($t=-1$). This population is decreasing during the STIRAP process and vanishes afterwards.

While we have considered equal scattering lengths occurring accidentally in ^{87}Rb , this is not exactly valid and also not the generic situation applicable to other condensed elements. It could be imagined that the imbalance of mean-field shifts deteriorates the transfer efficiency due to a violation of the bare two-photon resonance condition. Still, one could apply a time-dependent detuning that rectifies this effect in order to achieve an optimal adiabatic passage. Such a strategy has been proposed in Refs. [22,24].

However, we have studied numerically the situation of unequal scattering lengths without modifying the detunings and found no adverse effects. First, we have examined the efficiency of the transfer procedure using the real scattering data of the JILA experiment [33,34] for the trapped hyperfine states $|b\rangle \equiv |F=1, m_F=-1\rangle$ and $|c\rangle \equiv |2, 1\rangle$. Using the scattering parameters $(a_{bb}, a_{bc}, a_{cc}) = 104 a_0(1.03, 1, 0.97)$, there is an almost complete transfer to the rotational state possible, yielding essentially identical curves as shown in Figs. 2–4. However, there are slightly higher excitations than in the idealized case. Second, we find that even a drastic variation of the scattering lengths does not spoil the transfer efficiency. It only leads to a further increase of the “breathing” of the vortex. As an example, we depict the results of the simulations for a vanishing cross-component scattering length $(a_{bb}, a_{bc}, a_{cc}) = 104 a_0(1.03, 0, 0.97)$ in Figs. 5 and 8. Once more, these simulations confirm the remarkable robustness of the STIRAP scheme.

A. The two-component Thomas-Fermi approximation

The Thomas-Fermi (TF) limit is an extremely useful approximation for the ground state of an interacting BEC.

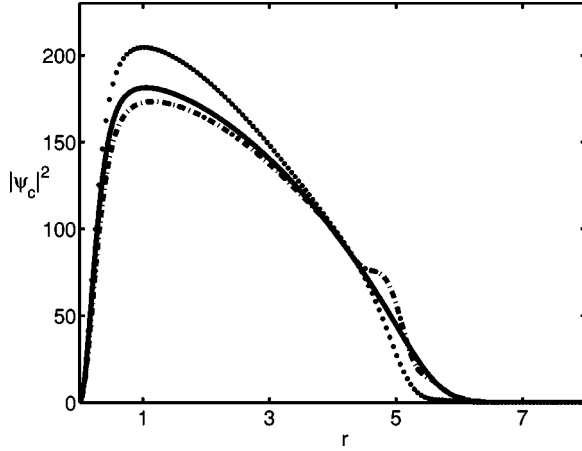


FIG. 5. Time evolution of the vortex state density $|\psi_c(r, t)|^2$ vs radius r measured in units of a_{HO} . In this simulation the self-scattering lengths of ^{87}Rb were chosen, but a_{bc} was deliberately set to zero. This change gives rise to an increase of the residual excitations of the final vortex state while the transfer efficiency again is higher than 99%. The dashed and dotted lines show the “breathing” of the vortex state at different times t . As a reference, the solid line depicts the stationary vortex state.

Where applicable, it simply disregards the kinetic energy contribution to the total system energy. This is also possible for an excited vortex state. We will now consider this TF approximation for the two ground-state components, after adiabatically eliminating the ψ_a component,

$$\psi_a(r, t) \approx -\frac{\Omega_p(t)}{\Delta} \psi_b - \frac{r \Omega_d(t)}{\Delta} \psi_c, \quad (23)$$

in order to obtain a simple estimate. During the adiabatic passage, the irrotational state ψ_b shall be transformed coherently into the vortex state ψ_c . Thus, the relevant Hamiltonian in the reduced two-state manifold reads

$$H_{\text{TF}}(t) = \frac{r^2}{2} + \kappa n(r) - \begin{pmatrix} \frac{|\Omega_p(t)|^2}{\Delta} & \frac{\Omega_d(r, t) \Omega_p^*(t)}{\Delta} \\ \frac{\Omega_d^*(r, t) \Omega_p(t)}{\Delta} & \frac{|\Omega_d(r, t)|^2}{\Delta} - \frac{1}{2r^2} \end{pmatrix}. \quad (24)$$

Once more, we want to assume an adiabatic following condition to obtain a stationary solution of $\psi(r, t) = \exp[-i \int_{-\infty}^t d\tau \mu_{\text{TF}}(\tau)] (\psi_b(r), \psi_c(r))^T$. By solving the simple ensuing eigenvalue problem of Eq. (24), we find for the chemical potential in the vortex branch that

$$\mu_{\text{TF}} = \frac{r^2}{2} + \kappa n_{\text{TF}} + \delta\mu, \quad (25)$$

$$\delta\mu = \frac{1}{2\Delta} \left[\frac{\Delta}{2r^2} - |\Omega_d|^2 - |\Omega_p|^2 + \sqrt{|\Omega_d|^4 - 2|\Omega_d|^2 \left(\frac{\Delta}{2r^2} - |\Omega_p|^2 \right) + \left(\frac{\Delta}{2r^2} + |\Omega_p|^2 \right)^2} \right]. \quad (26)$$

To keep the notation simple, we have dropped all the spatial and temporal arguments. Vice versa, one has to determine the chemical potential μ_{TF} such that $N = 2\pi \int_0^\infty dr r n_{\text{TF}}$ is satisfied at each instant of the adiabatic passage. For the vortex component of the corresponding eigenvector, one finds

$$\begin{pmatrix} \psi_b \\ \psi_c \end{pmatrix} = \sqrt{n_{\text{TF}}} \begin{pmatrix} \cos \theta \\ \sin \theta \end{pmatrix}, \quad (27)$$

$$\tan \theta = \frac{\Re(\Omega_p^* \Omega_d)}{\Delta \left(\frac{1}{2r^2} - |\Omega_d|^2 - \delta\mu \right)}. \quad (28)$$

It turns out that the chemical potential is almost constant during the transfer process. Hence, we can choose the value of μ_{TF} for the TF solution of the vortex state, i.e.,

$$\mu_{\text{TF}} = \mu_{\text{TF}}(\Omega_{p,d} = 0) \approx \frac{r^2}{2} + \frac{1}{2r^2} + \kappa n_{\text{TF}} = \text{const.} \quad (29)$$

As shown in Fig. 3, the adiabatic evolution of these simple approximations matches the exact numerical results for the vortex state well. It should be pointed out that in our TF approximation we did not neglect the centrifugal term $1/2r^2$ in Eq. (24), which is actually also part of the kinetic energy. It is responsible for the vanishing density in the center of the vortex core. This turns out to be the better approximation for $t \geq 0$, while for $t < 0$, dropping the centrifugal potential provides the more accurate approximation because of the irrotational nature of the initial state.

B. Total energy of the system

The total energy of a BE condensed system can be obtained from the expectation value of the microscopic Hamiltonian with respect to a symmetry-broken ensemble [37,38], thereby discarding higher order correlation functions. Unless time-translational symmetry is broken due to explicit time dependencies of external fields, the total energy of the system must be conserved. Within these assumptions, the energy functional is given by

$$E = E_{\text{kin}} + E_{\text{TF}} + E_{\text{dip}}, \quad (30)$$

where the individual contributions are as follows:

$$E_{\text{kin}} = \pi \int_0^\infty dr r [|\partial_r \psi_a|^2 + |\partial_r \psi_b|^2 + |\partial_r \psi_c|^2], \quad (31)$$

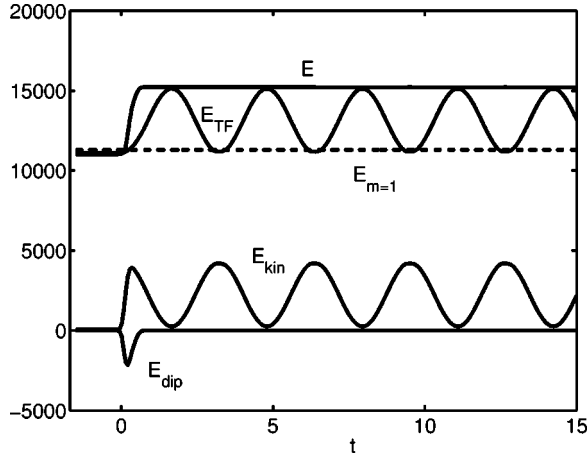


FIG. 6. Total energy E (measured in units of $\hbar\omega$) as a function of the time t (in natural units T_{HO}). The different contributions to the total energy are shown in the plot. $E_{m=1}$ denotes the energy of the condensate in the stationary vortex state. Because of remaining excitations the potential and kinetic energy oscillate. However, the total energy is conserved before and after the transfer process.

$$E_{\text{TF}} = \pi \int_0^\infty dr r \left[2\Delta |\psi_d|^2 + r^2 (|\psi_a|^2 + |\psi_b|^2 + |\psi_c|^2) + \frac{1}{r^2} |\psi_c|^2 + \kappa (|\psi_b|^2 + |\psi_c|^2)^2 \right], \quad (32)$$

and

$$E_{\text{dip}} = 2\pi \int_0^\infty \mathbf{d}r r [\psi_a^* \Omega_p \psi_b + \psi_a^* r \Omega_d \psi_c + \text{c.c.}]. \quad (33)$$

Equation (31) denotes the radial kinetic energy E_{kin} , while Eq. (32) represents all the energy arising from the detuning, the trap potential, and the mean-field shifts, respectively. The dipole energy, which is caused by the dipole coupling of the laser fields to the atoms, is given by the expression in Eq. (33).

The evolution of the total energy and its individual contributions is shown during the nonequilibrium transfer in Fig. 6. As expected, the total energy is constant before and after the STIRAP process. However, due to an excitation of the breathing mode, the kinetic as well as the potential energy exhibit complementary oscillations. The dipole energy is negative, which is well known from the interaction of a two-level atom with a laser field. This is due to the fact that the polarization of the atom is counteracting the external electromagnetic field.

C. Linear response of the system and breathing modes

The numerical simulations show that a transfer of almost 100% of the particles into a vortex state is possible. Still, residual radial excitations of the vortex state remain. As the frequency of these radial excitation is exactly twice the radial harmonic trapping frequency, $\varepsilon = 2\omega$, it must be related to the scaling symmetry of the two-dimensional system. These

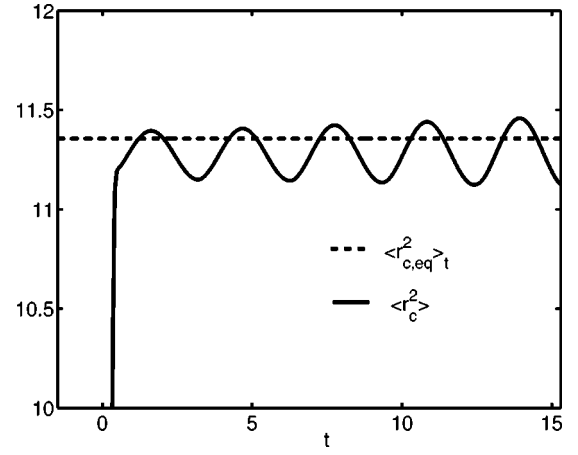


FIG. 7. Mean squared radius $\langle r_c^2 \rangle_t$ of the vortex state vs time (measured in units of a_{HO} and T_{HO} , respectively). Before the transfer process this state is not occupied. Afterwards the mean squared radius oscillates around the equilibrium value $\langle r_{c,\text{eq}}^2 \rangle$ (dashed line). The frequency of the excitation is exactly 2ω .

“breathing modes” have been studied first theoretically in Refs. [43,44] and experimentally in Ref. [45].

The mechanism for exciting these modes arises from squeezing the harmonic potential in time. In the present context of the STIRAP configuration, the origin of such an additional potential can be understood from considering Eq. (24). During the turn-on of the laser fields, we induce an ac-Stark-shift potential $|\Omega_d(r,t)|^2/\Delta$, which is proportional to r^2 . While this effect is interesting by itself, it could be eliminated easily by an appropriate control of the trapping potential, thus reducing the amount of excitations.

Moreover, a completely adiabatic transfer is limited by two factors: On the one hand a standard STIRAP process in a homogeneous gas requires an adiabaticity condition $\Omega\tau \gg 1$, i.e., the time delay τ must be sufficiently large. On the other hand τ cannot be chosen arbitrarily large because here we deal with a STIRAP process in a trap. Therefore, coupling to external motion has to be taken into consideration for large time delays τ .

The residual radial excitations can be visualized by evaluating the mean squared radius

$$\langle r_c^2 \rangle_t = \frac{2\pi}{N} \int_0^\infty dr r \psi_c(r,t)^* r^2 \psi_c(r,t), \quad (34)$$

which is proportional to the potential energy of the vortex component. As shown in Fig. 7, this quantity is oscillating with the frequency $\varepsilon = 2\omega$, which corresponds to the breathing mode (see Fig. 8).

In addition, small radial excitations (i.e., the linear response) of a BEC can be understood from Bogoliubov theory [40,41]. Therefore, we now consider the radial one-component GP equation for the vortex state with angular momentum $1\hbar$ that reads

$$i\partial_t \psi(r,t) = (h^{(1)} + \kappa |\psi(r,t)|^2) \psi(r,t), \quad (35)$$

with $h^{(1)}$ defined in Eq. (22). With the ansatz

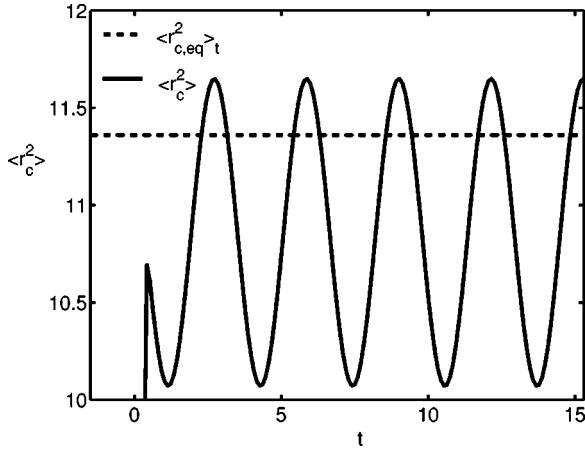


FIG. 8. Mean squared radius $\langle r_c^2 \rangle_t$ of the vortex state vs time (measured in units of a_{HO} and T_{HO} , respectively). In this simulation the self-scattering lengths of ^{87}Rb were chosen, but a_{bc} was deliberately set to zero. This change corresponds to an increase of the “breathing” of the final vortex state.

$$\psi(r, t) = e^{-i\mu t} (\psi_0(r) + u(r)e^{-i\epsilon t} + v^*(r)e^{i\epsilon t}), \quad (36)$$

where $\psi_0(r)$ is the wave function of the stationary vortex, the time evolution of which is determined by the chemical potential μ , and $u(r)$ and $v(r)$ denote the excitation modes with the normalization ($\epsilon > 0$)

$$2\pi \int_0^\infty dr r [|u(r)|^2 - |v(r)|^2] = 1. \quad (37)$$

The spectrum can be calculated from the linear response eigenvalue problem

$$\begin{pmatrix} h & \kappa \psi_0^2 \\ -\kappa \psi_0^{*2} & -h^* \end{pmatrix} \begin{pmatrix} u(r) \\ v(r) \end{pmatrix} = \epsilon \begin{pmatrix} u(r) \\ v(r) \end{pmatrix}, \quad (38)$$

where

$$h = h^{(1)} - \mu + 2\kappa |\psi_0(r)|^2. \quad (39)$$

The results of our numerical calculations are shown in Figs. 9 and 10, being in agreement with earlier work [42]. The lowest mode ($p=0$) corresponds to the condensate wave function itself (Goldstone mode). The frequency spectrum can be compared to spectrum of the well-known two-dimensional quantum-mechanical harmonic oscillator, which is given by

$$\epsilon_{\text{HO}} = 2p + |m| + 1, \quad (40)$$

where $p \in \mathbb{N}$ denotes the principal quantum number, $m \in \mathbb{Z}$ denotes the angular momentum, and in our case, $|m|=1$ is fixed.

IV. CONCLUSIONS

In this paper, we have developed a novel scheme for the optical creation of vortices in a trapped Bose-Einstein condensate, using the technique of stimulated Raman adiabatic

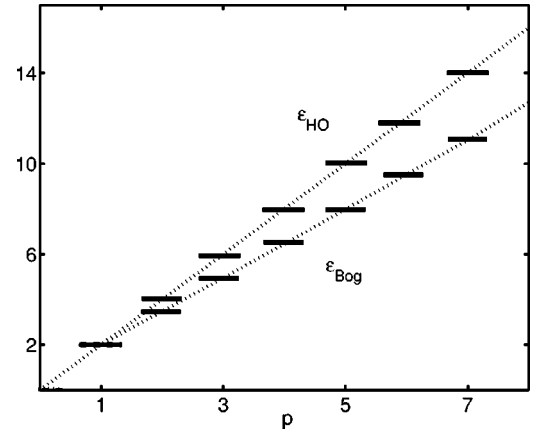


FIG. 9. Excitation frequencies ϵ relative to the ground state frequency of a quasi-two-dimensional BEC in the vortex state ($|m|=1$) measured in units of ω , in comparison to the two-dimensional harmonic oscillator with fixed $|m|=1$. For $p=0$ and $p=1$ the linear and nonlinear energies are identical. For $p \geq 2$ they split, and the excitation energies of the BEC lie below those of the noninteracting gas.

passage (STIRAP). In our model, we considered a BEC of three-level atoms in a Λ -configuration of the electronic states, which are coupled by two copropagating laser pulses. The aim was the transfer of angular momentum, carried by one of the beams (Gauss-Laguerre mode), to the BEC. The underlying mechanism of STIRAP is analogous to single-particle physics. In contrast to the latter case, we derived a multicomponent nonlinear Schrödinger equation (Gross-Pitaevskii equation), using the mean-field approximation. We presented results of numerical simulations that apply to a BEC of ^{87}Rb atoms. For a suitable set of laser parameters an almost 100% transfer to the vortex state can be achieved. These results can be understood with an intuitive and accurate approximation within the Thomas-Fermi limit. The occurrence of residual radial excitations in the vortex state can be explained by so-called breathing modes, which are spe-

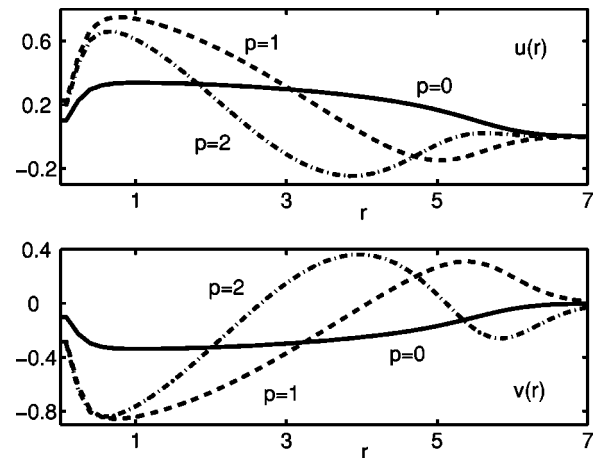


FIG. 10. Excitation modes obtained by Bogoliubov theory. The first three modes of $u(r)$ and $v(r)$ are plotted. The lowest mode ($p=0$) corresponds to the condensate wave function itself (Goldstone mode).

cific for the two-dimensional regime and can be eliminated by an appropriate control of the trap frequency. To confirm these explanation, we have calculated the Bogoliubov excitation spectrum numerically.

ACKNOWLEDGMENTS

We would like to acknowledge fruitful discussions with Bruce W. Shore and Karl-Peter Marzlin.

-
- [1] A. Fetter, *J. Low Temp. Phys.* **129**, 263 (2002), and references therein.
- [2] J. Williams and M. Holland, *Nature (London)* **401**, 568 (1999).
- [3] M. Matthews, B. Anderson, P. Haljan, D. Hall, C. Wieman, and E. A. Cornell, *Phys. Rev. Lett.* **83**, 2498 (1999).
- [4] K. Madison, F. Chevy, W. Wohlleben, and J. Dalibard, *Phys. Rev. Lett.* **84**, 806 (2000).
- [5] K. Madison, F. Chevy, V. Bretin, and J. Dalibard, *Phys. Rev. Lett.* **86**, 4443 (2001).
- [6] J. Abo-Shaer, C. Raman, J. Vogels, and W. Ketterle, *Science* **292**, 476 (2001).
- [7] P. C. Haljan, I. Coddington, P. Engels, and E. A. Cornell, *Phys. Rev. Lett.* **87**, 210403 (2001).
- [8] P. Engels, I. Coddington, P. C. Haljan, V. Schweikhard, and E. A. Cornell, *Phys. Rev. Lett.* **90**, 170405 (2003).
- [9] K. Madison, F. Chevy, W. Wohlleben, and J. Dalibard, *J. Mod. Opt.* **47**, 2715 (2000).
- [10] P. Engels, I. Coddington, V. Schweikhard, and E. A. Cornell, *J. Low Temp. Phys.* **134**, 683 (2004).
- [11] L. Dobrek, M. Gajda, M. Lewenstein, K. Sengstock, G. Birkl, and W. Ertmer, *Phys. Rev. A* **60**, R3381 (1999).
- [12] J. Denschlag *et al.*, *Science* **287**, 97 (2000).
- [13] H. Pu, S. Raghavan, and N. Bigelow, *Phys. Rev. A* **63**, 063603 (2001).
- [14] B. Damski, Z. P. Karkuszewski, K. Sacha, and J. Zakrzewski, *Phys. Rev. A* **65**, 013604 (2002).
- [15] R. A. Beth, *Phys. Rev.* **50**, 115 (1936).
- [16] *Lasers*, edited by P. Miloni and J. Ebery (Wiley-Interscience, New York, 1988).
- [17] S. J. van Enk and G. Nienhuis, *Europhys. Lett.* **25**, 497 (1994).
- [18] L. Allen, M. Beijersbergen, R. Spreeuw, and J. Woerdman, *Phys. Rev. A* **45**, 8185 (1992).
- [19] H. He, M. Friese, N. Heckenberg, and H. Rubinsztein-Dunlop, *Phys. Rev. Lett.* **75**, 826 (1995).
- [20] S. Kuppens, M. Rauner, M. Schiffer, K. Sengstock, W. Ertmer, F. van Dorsselaer, and G. Nienhuis, *Phys. Rev. A* **58**, 3068 (1998).
- [21] S. Gspann, A. Meyer, S. Bernet, and M. Ritsch-Marte, *J. Acoust. Soc. Am.* **115**, 1142 (2004).
- [22] K.-P. Marzlin, W. Zhang, and E. M. Wright, *Phys. Rev. Lett.* **79**, 4728 (1997).
- [23] E. Bolda and D. Walls, *Phys. Lett. A* **246**, 32 (1998).
- [24] R. Dum, J. I. Cirac, M. Lewenstein, and P. Zoller, *Phys. Rev. Lett.* **80**, 2972 (1998).
- [25] K. Bergmann, H. Theuer, and B. W. Shore, *Rev. Mod. Phys.* **70**, 1003 (1998).
- [26] E. Arimondo and G. Orriols, *Nuovo Cimento Soc. Ital. Fis., A* **17A**, 333 (1976).
- [27] E. Arimondo, *Prog. Opt.* **35**, 259 (1996), and references therein.
- [28] S. Harris, J. Field, and A. Imamoglu, *Phys. Rev. Lett.* **64**, 1107 (1990).
- [29] L. Hau, S. Harris, Z. Dutton, and C. Behroozi, *Nature (London)* **397**, 594 (1999).
- [30] G. Juzeliunas, M. Masalas, and M. Fleischhauer, *Phys. Rev. A* **67**, 023809 (2003).
- [31] A. Parkins, P. Marte, P. Zoller, and J. Kimble, *Phys. Rev. Lett.* **71**, 3095 (1993).
- [32] R. Walser, J. I. Cirac, and P. Zoller, *Phys. Rev. Lett.* **77**, 2658 (1996).
- [33] M. R. Matthews, D. S. Hall, D. S. Jin, J. R. Ensher, C. E. Wieman, and E. A. Cornell, *Phys. Rev. Lett.* **81**, 243 (1998).
- [34] D. S. Hall, M. R. Matthews, J. R. Ensher, C. E. Wieman, and E. A. Cornell, *Phys. Rev. Lett.* **81**, 1539 (1998).
- [35] Th. Busch, J. I. Cirac, V. M. Pérez-García, and P. Zoller, *Phys. Rev. A* **56**, 2978 (1997).
- [36] F. Dalfovo, S. Giorgini, L. P. Pitaevskii, and S. Stringari, *Rev. Mod. Phys.* **71**, 463 (1999).
- [37] R. Walser, J. Cooper, and M. Holland, *Phys. Rev. A* **63**, 013607 (2001).
- [38] *Quantum Theory of Finite Systems*, edited by J.-P. Blaizot and G. Ripka (MIT Press, Cambridge, MA, 1986).
- [39] *Quantum Optics in Phase Space*, edited by W. P. Schleich (Wiley-VCH, Berlin, 2001).
- [40] N. Bogoliubov, *J. Phys. (Moscow)* **11**, 23 (1947).
- [41] A. L. Fetter, *Ann. Phys. (N.Y.)* **70**, 67 (1972).
- [42] T. Isoshima and K. Machida, *Phys. Rev. A* **59**, 2203 (1999).
- [43] L. P. Pitaevskii, *Phys. Lett. A* **221**, 14 (1996).
- [44] Yu. Kagan, E. L. Surkov, and G. V. Shlyapnikov, *Phys. Rev. A* **54**, R1753 (1996).
- [45] F. Chevy, V. Bretin, P. Rosenbusch, K. W. Madison, and J. Dalibard, *Phys. Rev. Lett.* **88**, 250402 (2002).